Available online at www.sciencedirect.com
ScienceDirect
Geochimica et Cosmochimica Acta 70 (2006) 5356–5370
Geochimica
www.elsevier.com/locate/gca

Origin of ore fluids in the Muruntau gold system: Constraints from noble gas, carbon isotope and halogen data

Torsten Graupner [a,d,*], Samuel Niedermann [b], Ulf Kempe [c], Reiner Klemd [d,e], Achim Bechtel [f]

[a] Federal Institute for Geosciences and Natural Resources (BGR), Stilleweg 2, 30655 Hannover, Germany
[b] GeoForschungsZentrum Potsdam, Telegrafenberg, 14473 Potsdam, Germany
[c] Institute of Mineralogy, TU Bergakademie Freiberg, Brennhausgasse 14, 09599 Freiberg, Germany
[d] Institute of Mineralogy, Universität Würzburg, Am Hubland, 97074 Würzburg, Germany
[e] Department of Geology, University of Johannesburg, Auckland Park 2006, South Africa
[f] Institute of Geosciences, Montan-Universität Leoben, Peter-Tunner-Strasse 5, 8700 Leoben, Austria

Received 9 March 2006; accepted in revised form 9 August 2006

Abstract

Hydrothermal vein minerals directly associated with native gold mineralization in the Muruntau vein system (Uzbekistan) have been studied for noble gas, carbon isotope and halogen chemistry of the trapped ore-related fluids. Helium trapped in early arsenopyrite 1, which has preserved the original fluid signature better than associated scheelite and quartz, indicates a small input from a mantle source (⩽5% of total He). However, the overwhelming majority of the He in the fluid (~95%) is from crustal sources. The noble gases Ne, Kr and Xe in the sample fluids are dominated by gases of atmospheric origin. The carbon isotope ($\delta^{13}C$: −2.1‰ to −5.3‰) and halogen characteristics of the fluids (log Br/Cl: −2.64 to −3.23) lend further support for the activity of juvenile fluids during the main ore stage. The high proportion of crustal components in the ore-forming fluids may be explained by intense fluid–rock interaction and is also supported by previous Nd and Sr isotope studies. The involvement of a juvenile fluid component during the main stage of hydrothermal activity at Muruntau (~275 Ma) can be linked to the emplacement of lamprophyric dikes at Muruntau, due to apparently overlapping ages for high-temperature alteration, related ore vein formation and intrusion of the dikes. The input of mantle-derived fluids, possibly related to the Hercynian collisional event in the western Tien Shan, stimulated intense fluid–rock interaction in the crust. In this context, the mantle-derived fluid should be considered as one possible carrier of metals. Significant amounts of external meteoric fluids circulating in fracture systems are interpreted to have modified the noble gas signature of fluid in quartz, mostly during late, low temperature fluid circulation.

1. Introduction

The late Paleozoic orogenic Au system at Muruntau (Western Uzbekistan; Fig. 1A) has been the subject of numerous scientific studies since its discovery in 1958. The majority of the work of the last decade was focused either on the structural setting of the ore-bearing system (e.g., Drew et al., 1996; Obraztsov, 2001; Khamrabaev et al., 2003; Wall et al., 2004), the age of magmatism, hydrothermal alteration and mineralization as well as their possible relations (e.g., Kostitsyn, 1996; Kempe et al., 2004; Morelli et al., 2004), the mineral associations in the ore veins including the isotope systematics of scheelite (e.g., Obraztsov, 1999; Kempe et al., 2001a; Vasilevskiy et al., 2004; Graupner et al., 2005), or the chemical composition of the hydrothermal fluids in the ore veins (e.g., Graupner et al., 2001; Wilde et al., 2001).

However, the genesis of this large ore system (>3400 t Au) remains controversial (e.g., Kotov and Poritskaya, 1992; Shayakubov et al., 1998; Obraztsov, 2001). Important fields of ongoing debate are the source(s) of the

* Corresponding author.
E-mail address: torsten84@gmx.de (T. Graupner).

0016-7037/$ - see front matter © 2006 Elsevier Inc. All rights reserved.
doi:10.1016/j.gca.2006.08.013

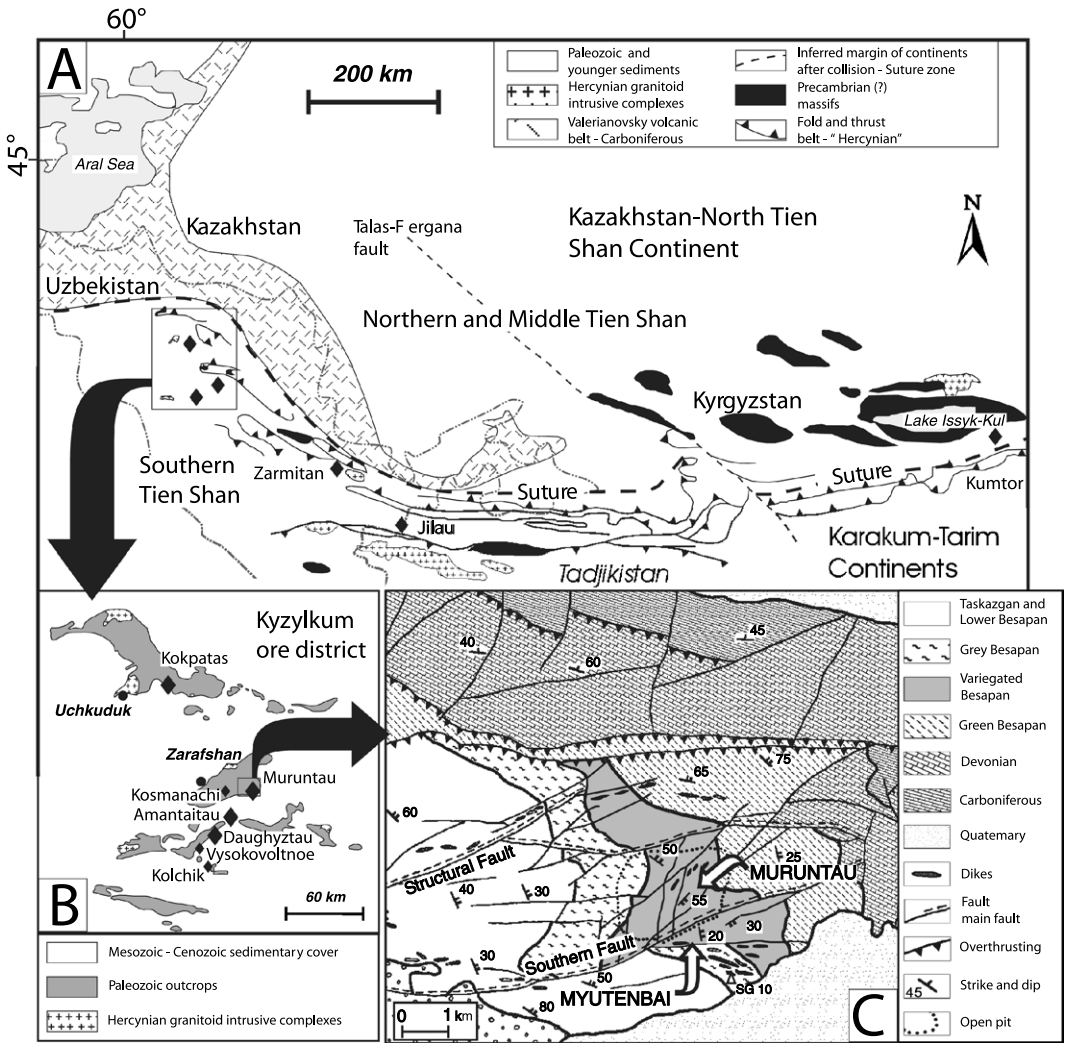

Fig. 1. Location of gold deposits (diamonds) within (A) the Tien Shan Mountains in Central Asia (from Zonenshain et al., 1990; Kotov and Poritskaya, 1992; Drew et al., 1996) and (B) the Central Kyzylkum ore district (e.g., Shayakubov et al., 1999). The schematic geological map of the Muruntau ore field (C) is modified after P.A. Ivanov (personal communication). The location of deep drill hole SG 10 is given by a white triangle.

Au-related hydrothermal fluids and the mechanisms of gold enrichment. Opinions range from a purely sedimentary origin of the solutions (e.g., Wilde et al., 2001) to metamorphic devolatilization of the underlying metasedimentary rocks, to a granite-related origin of the hydrothermal fluids (e.g., Kotov and Poritskaya, 1992), and to an influence of mantle- or plume-related sources on the evolution of the large hydrothermal system at Muruntau (e.g., Ivankin and Nasarova, 1991; Kremenetsky and Minzer, 1995; Kempe et al., 1997). Possible sources of the gold that have been discussed are carbonaceous rocks of the metasedimentary packages hosting Muruntau and a number of smaller Au and Au–Ag systems in the region (black shales, fossil placer occurrences, e.g., Bel'kova and Ognev, 1970; Garkovets, 1973; Voronkov et al., 1983), spatially associated Hercynian granitoids (e.g., Cole and Seltmann, 2000), underlying zones of metamorphism within the lower crust stimulated by mantle fluids (e.g., Mushkin and Jaroslavsky, 1974, 1976), and the uppermost part of the mantle (e.g., Ivankin and Nasarova, 1991). For each of the models, supporting geological and geochemical findings (e.g., stable isotope data) have been presented (e.g., Zakharevich et al., 1987—$\delta^{34}S$ and $\delta^{13}C$ data; Berger et al., 1994—$\delta^{34}S$, δD and $\delta^{18}O$ data; Zairi et al., 1995—$\delta^{13}C$ data).

We report here new noble gas (He, Ne, Ar, Kr and Xe), carbon isotope, and halogen data for hydrothermal ore fluids from Muruntau, which were obtained to constrain the source(s) of the economic Au mineralization. The studied quartz, arsenopyrite and scheelite derive from relatively high-grade auriferous zones, which include steeply dipping lenticular, vein-like quartz bodies (so-called central veins) and enveloping stockworks. The data will be discussed considering geological field observations as well as published results [e.g., recently published radiometric age data for magmatic rocks and vein minerals by Morelli et al. (2004) and Kempe et al. (2004)] in order to provide new constraints on the formation conditions of this large gold-bearing hydrothermal system.

2. Geological setting of the Muruntau system

The Muruntau Au system is located in the Central Kyzylkum district in Uzbekistan, a sub-province of the Southern Tien Shan belt Au province as defined by Kudrin et al. (1990); compare Fig. 1A–B. Based on occurrences of mafic rocks of ophiolite association (e.g., Kotov and Poritskaya, 1992), a Hercynian collisional suture separating the Kazakhstan-North-Tien Shan Continent and the Karakum-Tarim Continent may be assumed ~150 km to the northeast of Muruntau (cf. Zonenshain et al., 1990; Drew et al., 1996). This suture zone, which has been contested by some authors (e.g., Wilde and Gilbert, 1999), separates the fold and thrust belt of the Southern Tien Shan from the Middle Tien Shan (e.g., Yakubchuk et al., 2002).

The southern Tamdytau Mountains in the Central Kyzylkum, which host Muruntau and a number of smaller Au (e.g., Myutenbai) and Au–Ag occurrences (e.g., Kosmanachi—Fig. 1B–C), are mainly composed of metasedimentary rocks of the Taskazgan (Middle Proterozoic?—Lower Ordovician) and the Besapan suites (Ordovician—Silurian). Published age data for the predominantly monotonous packages involving metasiltstones and shales, with interbeds of sandstone, are scarce. Kim (1970); in (Mansurov et al., 1991) determined an Upper Proterozoic Pb/Pb model age of 870 ± 20 Ma for carbonates of the Taskazgan suite. Bukharin et al. (1984) interpreted the fossil content of the upper "Variegated Besapan", which is underlain by the Grey and Black (Lower) Besapan and overlain by the Green Besapan (Fig. 1C), as a result of a tectonic mixture. The age of the regional metamorphism (green-schist facies at late stages) is constrained by K–Ar and Rb–Sr dating. Loshchinin et al. (1986) reported 410 and 430 Ma K–Ar ages for the Taskazgan. Kostitsyn (1996) determined Rb–Sr whole rock and density fraction isochron ages of 403 ± 18 and 393 ± 26 Ma for two drill core samples of (unaltered) Black Besapan and Green Besapan, respectively. The overthrust structures in the southern Tamdytau area are sealed by a cover of Devonian to Lower Carboniferous carbonate shelf deposits (Mukhin et al., 1988; Fig. 1C).

The Au-ore hosting "Variegated Besapan" occurs in a lenticular form ("Muruntau lens", Mukhin et al., 1988) within the Besapan suite with a thickness of up to 2000 m. Pelitic rock types are interlayered with psammopelitic to psammitic packages of thin-to-medium layered nature in the "Variegated Besapan" (Wall et al., 2004). Based on the virtually ubiquitous enrichment of the "Variegated Besapan" in sulphides, these rocks were considered as a potential source of gold (Shayakubov et al., 1998). Possibly, fluids related to formation of hydrothermal veins at Muruntau could have overprinted these rocks as well, causing secondary sulphide formation.

The Muruntau deposit lies near the intersection of a major, regional antiformal hinge zone (Dzhambulak anticlinoid; Hercynian; D2 event of Yakubchuk et al., 2002) deformed by a regional Z-shaped structure and the Muruntau-Daughyztau fault zone (Kotov and Poritskaya, 1992). Sub-E-W-trending faults provide the space for a significant part of the large quartz bodies; the positions of the mineralized zones are often controlled by them (Obraztsov, 2001). Predominantly NE-trending fault/shear zones cut and offset the earlier structures and the auriferous mineralization (Fig. 2).

A number of overlying prograde and retrograde stages of alteration were identified at Muruntau; the early, high-temperature stage includes amphibole-pyroxene-, biotite- and microcline-bearing assemblages (cf. Arifulov, 1976; Uspenskiy and Aleshin, 1993; Kempe et al., 2002), whereas the medium-temperature stages are characterized by albite-, carbonate-apatite-, chlorite- and sericite-dominated alteration assemblages (e.g., several authors in Shayakubov et al., 1998; Kempe et al., 2002).

Intrusions of granite to granodiorite composition, exposed south-east and north-west of Muruntau, are of Hercynian age according to their tectonic positions and radiometric ages (e.g., Kotov and Poritskaya, 1992; Kostitsyn, 1996; Kempe et al., 2004). Intrusions of granodioritic dikes of the so-called Muruntau intrusive complex occur along sub-E-W-striking fault zones in the ore field and at intersections with other fault zones. Another type of post-orogenic dikes, possibly temporally separated from the granitic dikes, is composed of kersantites and lamprophyres. These rocks occur adjacent to the Muruntau deposit arranged into dike belts similar to the granitic dikes. The granitic intrusive body found closest to the Muruntau hydrothermal system is the Murun granite. It is exposed in the SG-10 borehole south-east of Muruntau (Fig. 1C; depth interval: from 4005 to 4296 m at final depth) and is strongly altered (Shayakubov et al., 1999). Wall rock alteration (biotitization and K-feldspatization, assumed to have been closely related to early ore formation) apparently overlaps in time with the intrusion of mafic dikes at ~275 Ma (Kostitsyn, 1996). There is also evidence for some later hydrothermal events of minor importance that have been dated at ~260, 230 and 220 Ma, respectively (Rb–Sr data, summarized in Kostitsyn (1996); Ar/Ar dating by Wilde et al. (2001)).

Early horizontal (so-called "flat") quartz veinlets in the "Variegated Besapan", which occur parallel to sub-parallel to the foliation of the host rocks, generally show slight enrichment in gold but are sub-economic (Khokhlov, 1990; Kempe et al., 2001a). The main economic gold resources occur in moderately to steeply south dipping (Wall et al., 2004) columnar structures, which were defined as "ore columns" (Shayakubov et al., 1999). These structures are composed of mineralized stockworks that sometimes envelop large lenticular, steeply dipping, vein-like and high-grade auriferous quartz bodies—the so-called central veins (e.g., Golovanov et al., 1988, 1998b; Graupner et al., 2005; Fig. 2).

In these high-grade auriferous vein structures and the stockworks, two main mineral associations can be distinguished. Initially, early minerals including early quartz

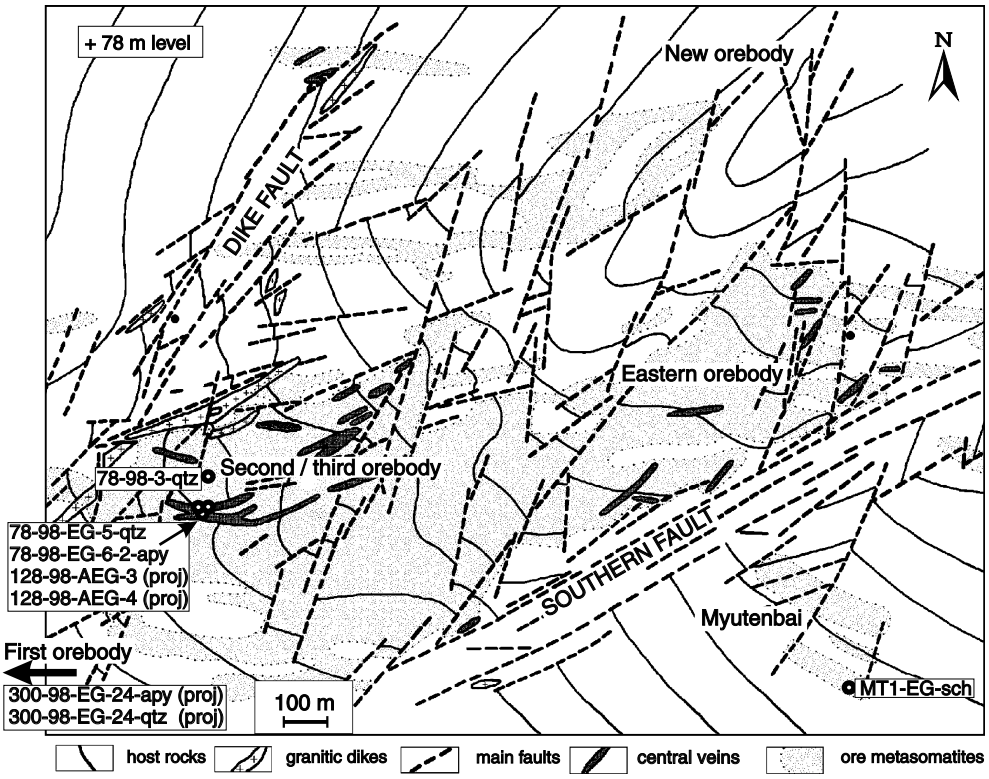

Fig. 2. Schematic sketch of the orebodies of the Muruntau deposit including Myutenbai. The layering of the host rocks is schematically shown by solid lines. The locations of the analyzed samples are shown. Samples 300-98-EG-24 as well as 128-98-AEG-3 and -4 are from the +300-and +128-m mining levels, respectively; however, the locations of the latter two samples have been projected vertically to the +78-m level. The position of 300-98-EG-24 outside the map area (within the first orebody) is indicated by an arrow.

(Graupner et al., 2005), scheelite (Kempe et al., 2001a), allanite, monazite, rutile (Kempe et al., 2001b), arsenopyrite 1, and Bi-tellurides (Graupner et al., 2005) have formed euhedral crystals. These were brecciated in, probably, several stages and now occur as angular fragments cemented partly by deformed quartz or by later, essentially undeformed minerals (Graupner et al., 2000; Kempe et al., 2001b; Graupner et al., 2005). Due to their small size (about 10–30 μm in diameter), Au 1 grains associated with early deformed quartz were not significantly affected by the brecciation. Later mineral assemblages in the veins include late quartz, Mg-chlorite, sericite, calcite, dolomite, pyrite and apatite. These mineral assemblages may be related to the stages of high temperature (biotitization and K-feldspatization) and medium temperature alteration (albitization, serizitization and chloritization) of the wall rocks, respectively (Graupner et al., 2005). Arsenopyrite 2 predominantly occurs in veinlets that cross-cut the earlier ore mineralization and was not studied further here.

3. Samples and experimental techniques

Eight of the studied samples come from two mining levels (+78 m; +128 m) of shaft M of the Muruntau mine including its south-eastern extension into the Myutenbai deposit (only at level +78 m; Fig. 2). During sample preparation, separation of the quartz types was not possible because they can only be distinguished using CL microscopy (Graupner et al., 2000). Therefore, quartz types are not further specified in the present study. Five quartz samples and one early arsenopyrite 1 sample were derived from steeply dipping central vein structures at Muruntau (Fig. 2); the arsenopyrite 1 is from a lens-like structure within the northern marginal part of the vein. The vein quartz is low in sulphides, contains variable amounts of native gold [early euhedral Au 1 and, sometimes, later anhedral Au 2; see Graupner et al. (2005) for details], and is recrystallized to variable degrees. Arsenopyrite 1 is deformed and contains inclusions of Au 1-type, Ag-poor gold (9.6–12.8 wt% Ag; Fig. 3) and—more rarely—of native Bi. An additional quartz sample is from a poorly recrystallized stockwork veinlet from the central part of the Muruntau mine. The brownish, deformed scheelite, which is associated with Au 1 mineralization in time and space [scheelite 2 of Uspenskiy and Aleshin (1993) and Kempe et al. (2001a)], is derived from a main quartz vein at Myutenbai (+78 m), which is similar in appearance to the Muruntau central veins.

Two samples (one of quartz and one of early arsenopyrite 1) come from the +300 m level of the Muruntau open pit. Both samples are from a quartz-arsenopyrite 1 stockwork veinlet. Here, the arsenopyrite 1 is concentrated in the central part of the veinlet. In this part of the open pit, mining is continuously carried out; therefore, the samples did probably not spend a long time at the surface.

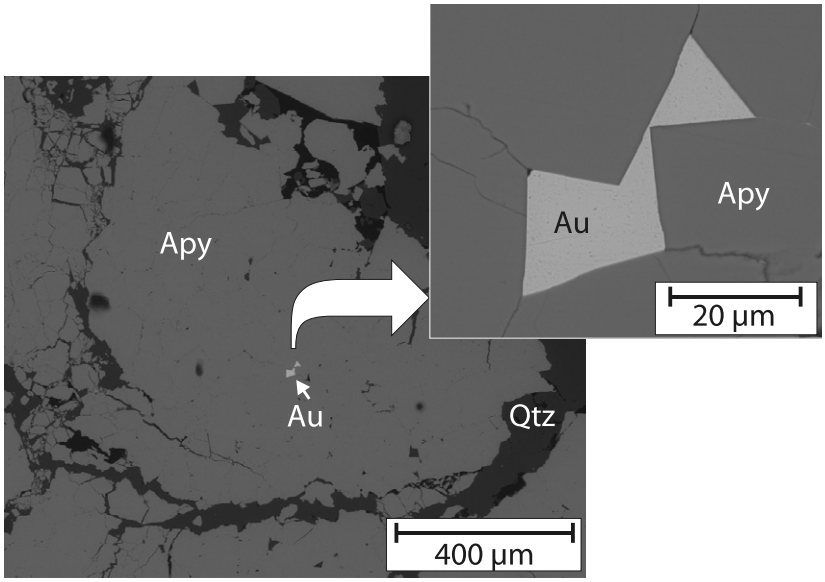

Fig. 3. BSE image of arsenopyrite 1 (sample 78-98-EG-6-2-apy) from a central quartz vein from Muruntau (second/third orebody). Arsenopyrite 1 is deformed and contains inclusions of a Au 1-type, Ag-poor gold. Apy, arsenopyrite 1; Qtz, quartz.

The genetic types of the fluid inclusions contained in the quartz and scheelite from the ore veins investigated in this study, as well as their salinity and major cation–anion compositions, have already been described in detail elsewhere (Graupner et al., 2001, 2005) and, thus, are summarized here only briefly. The early quartz contains variable proportions of early, probably primary/pseudosecondary (P/PS), CO_2-bearing aqueous, high-temperature [temperature of total homogenization (T_h) $\leqslant \sim 400$ °C] and later, at least partly CO_2-bearing, aqueous fluid inclusions (often low-density inclusions). Increased numbers of late aqueous, low-temperature inclusions ($T_h < 250$ °C) generally occur towards the vein margins. Scheelite seems to be more resistant to recrystallization and alteration and/or extinction of trapped early fluids than the coexisting quartz, as indicated by the distribution characteristics of probably P/PS inclusions. The CO_2 contents in P/PS inclusions in early quartz from the vein types studied here range from ~3 to ~15 mol% (non-H_2O volatiles (total): ~4 to ~17 mol%; CO_2/CH_4 ratios are between ~1 and ~13 (bulk gas chromatographic data)). Fluid phase separation is indicated for Au 2-bearing quartz from the central quartz veins.

3.1. Noble gas analysis

Samples of 0.6–1.5 g were loaded one at a time into an ultrahigh vacuum crusher and baked at 100 °C for 24 h. The gases were then released from fluid inclusions by squeezing the mineral grains between two hard-metal jaws, and noble gas concentrations and isotopic compositions were determined in a VG 5400 mass spectrometer. Crushing efficiency is estimated between 50% and 100%. Blanks were measured before each sample extraction and were $\sim 8 \times 10^{-12}$ cm^3 ^{4}He, $(5\text{–}10) \times 10^{-12}$ cm^3 ^{20}Ne, $(6\text{–}40) \times 10^{-11}$ cm^3 ^{40}Ar, $(1.4\text{–}7) \times 10^{-14}$ cm^3 ^{84}Kr, and $(7\text{–}40) \times 10^{-15}$ cm^3 ^{132}Xe. The mass spectrometer sensitivity and the isotopic mass discrimination were determined using the GFZ lab standard, an artificial mixture of the five noble gases with a ^{3}He/^{4}He ratio of $21.66 \pm 0.24 \times 10^{-6}$ and atmospheric isotopic compositions for Ne, Ar, Kr and Xe. All data have been corrected for analytical blanks, isobaric interferences (^{20}Ne, ^{22}Ne, ^{36}Ar and ^{38}Ar), and mass discrimination effects. Error limits correspond to the 95% confidence level; they include statistical uncertainties of the measurement, uncertainties of sensitivity and mass discrimination determinations, as well as blank and interference corrections. Further information about the gas purification line and the mass spectrometer, as well as on the analytical methods used, can be found in Niedermann et al. (1997). Noble gas data were obtained for five vein quartz, two arsenopyrite 1, and one scheelite sample.

3.2. Carbon isotopes

Samples of mostly ~4 g were loaded into a Pt crucible. CO_2 and H_2O released from the quartz by thermal decrepitation at 1000 °C under vacuum were trapped at liquid nitrogen temperature. Carbon dioxide was separated from H_2O at −78 °C (dry ice/methanol) and was frozen into glass tubes for mass spectrometric analyses. C-isotope determinations were carried out on a VG Sira-9 instrument (triple-collector, 90°, 9 cm radius). The $^{13}C/^{12}C$ isotope ratio of the CO_2 from a sample is compared with the corresponding ratio of an internal laboratory reference material (carbon dioxide gas), calibrated against the PDB standard. The reproducibility of the total analytical procedure is in the range of 0.1–0.2‰ for $\delta^{13}C$. Carbonatite (NBS-18) and limestone (NBS-19) standards were used

for control of the analytical results. The accuracy of the results is in the range of ±0.2‰. Carbon isotopes were determined for fluids trapped in five vein quartz samples.

3.3. Halogen geochemistry

Halide data (Br^- and Cl^- concentrations, Br/Cl ratios) were obtained by combined gas and ion chromatographic (GC/IC) analysis of quartz and scheelite samples at the F. Gordon Smith Fluid Incl. Lab., Department of Geology, University of Toronto (sample mass: ~1.2 g). After volatile analysis (Hewlett-Packard 5890 gas chromatograph with in-series photo-ionization and thermal conductivity detectors), the crushed samples are removed from the stainless steel crushers and leached with deionized water to produce leachate solutions, which are filtered and analyzed by IC (Bray et al., 1991; Channer et al., 1999). Calibration of the GC is carried out using a 0.5 ml injection of H_2O saturated air at known temperature and pressure, and 25 µl injections of CH_4–CO_2-bearing and C_2H_4-bearing standard gas mixtures (Channer et al., 1999). Propagated errors for calculated species concentrations in mmol/l range from 13% to 22%; the error on a Br/Cl ratio is estimated at 1.9% (Channer et al., 1999).

3.4. Trace element analysis of the host minerals

The trace element compositions of the quartz and arsenopyrite samples used for estimation of the *in situ* produced amounts of noble gases in the different minerals were determined by ICP mass spectrometry (Be: ICP-AES). For control of the analytical results the JA-3 andesite standard (Govindaraju, 1994) was used. The uncertainties on the trace element data are 5–10% (10% for REE data). Estimated conservative detection limits under the applied measurement conditions are 0.5 ppm for Li and Sr, 0.05 ppm for Ce and Pb, 0.02 ppm for La as well as 0.01 ppm for Pr, Nd, Gd, Sm, Th and U. The data for the scheelite sample were taken from Kempe and Oberthür (1997).

4. Results

4.1. Noble gases released by crushing

The results of noble gas (He, Ne, Ar, Kr and Xe) analysis of trapped fluids in quartz, scheelite and arsenopyrite 1 from central quartz vein and stockwork samples are listed in Table 1. The concentrations of ^{4}He range from 0.19 to 20.2×10^{-8} cm^3 STP g^{-1} for all studied minerals, and ^{40}Ar data are $5.1–33.6 \times 10^{-8}$ cm^3 STP g^{-1}. High concentrations of both noble gases occur in scheelite. The ^{40}Ar concentrations are similar in quartz and scheelite. Arsenopyrite 1 has lower ^{4}He and ^{40}Ar concentrations in fluid inclusions than the scheelite, but its ^{4}He values are higher than those for the quartz samples. Similar concentrations of ^{20}Ne, ^{84}Kr and ^{132}Xe were measured for fluids in quartz and scheelite ($475–1090 \times 10^{-12}$, $13.4–23.1 \times 10^{-12}$ and

Table 1
Noble gas isotope, carbon isotope and halogen compositions of trapped fluids in quartz, arsenopyrite 1 and scheelite from the Muruntau vein system

	^{4}He $\times 10^{-8}$ (cc STP/g)	^{20}Ne $\times 10^{-12}$ (cc STP/g)	^{40}Ar $\times 10^{-8}$ (cc STP/g)	^{84}Kr $\times 10^{-12}$ (cc STP/g)	^{132}Xe $\times 10^{-12}$ (cc STP/g)	^{3}He/^{4}He $\times 10^{-6}$	^{40}Ar/^{36}Ar	^{3}He/^{36}Ar $\times 10^{-6}$	^{4}He/^{40}Ar*	δ^{13}C (vs PDB)	Cl $\times 10^{16}$ (atoms/g)	log Br/Cl	^{40}Ar*/Cl $\times 10^{-6}$ #	Cl/^{36}Ar $\times 10^6$ #	CO_2/CH_4 (molar)
Scheelite 2															
MT1-EG-sch	20.2 ± 1.0	1087 ± 66	32.1 ± 1.6	17.5 ± 0.9	1.31 ± 0.09	0.033 ± 0.008	403.6 ± 1.6	8.5 ± 2.3	2.34 ± 0.17		10.8 ± 1.4	−2.88 ± 0.02	21.3	5.1	1.1 ± 0.1
Arsenopyrite 1															
78-98-EG-6-2-apy	5.18 ± 0.31	69.4 ± 4.3	5.10 ± 0.31	4.10 ± 0.25	0.48 ± 0.04	0.222 ± 0.027	307.4 ± 1.7	69 ± 10	26.3 ± 4.3						0.10 ± 0.01
300-98-EG-24-apy	6.30 ± 0.31	77.8 ± 4.1	6.15 ± 0.31	4.16 ± 0.56	0.60 ± 0.04	0.317 ± 0.066	356.2 ± 3.2	116 ± 26	6.01 ± 0.50						
Quartz															
300-98-EG-24-qtz	0.261 ± 0.013	1090 ± 56	33.6 ± 1.7	13.4 ± 1.1	1.61 ± 0.13	0.17 ± 0.14	498.3 ± 3.5	0.66 ± 0.55	0.0191 ± 0.0014						16.0 ± 1.3
128-98-AEG-3	0.188 ± 0.010	557 ± 28	27.4 ± 1.4	23.1 ± 1.9	1.86 ± 0.10	0.21 (+0.25/−0.21)	310.7 ± 1.9	0.45(+0.54/−0.45)	0.140 ± 0.019	−5.3 ± 0.2	4.20 ± 0.55	−2.64 ± 0.03	8.6	1.8	9.1 ± 0.7
128-98-AEG-4	0.571 ± 0.029	1006 ± 51	28.8 ± 1.7	19.9 ± 1.2	1.95 ± 0.11	0.14 ± 0.11	327.8 ± 1.4	0.91 ± 0.72	0.201 ± 0.017	−4.4 ± 0.2	11.5 ± 1.5	−2.91 ± 0.02	6.6	4.9	9.1 ± 0.7
78-98-EG-5-3	0.252 ± 0.013	475 ± 24	22.2 ± 1.3	16.1 ± 0.8	1.21 ± 0.07	0.26 ± 0.18	304.3 ± 1.3	0.90 ± 0.63	0.393 ± 0.064	−3.4 ± 0.2	3.60 ± 0.47	−2.87 ± 0.03	4.6	1.8	3.7 ± 0.3
78-98-EG-5-4	0.508 ± 0.025	707 ± 36	24.6 ± 1.2	14.0 ± 1.1	1.43 ± 0.12	0.108 ± 0.073	319.1 ± 1.4	0.71 ± 0.48	0.279 ± 0.024		4.30 ± 0.56	−2.76 ± 0.03	11.4	2.1	6.4 ± 0.5
78-98-EG-5-5												−2.76 ± 0.03			4.7 ± 0.4
78-98-3										−2.1 ± 0.2		−2.77 ± 0.03			4.1 ± 0.3

The accuracy of the values in these column is likely not better than a factor of 2 due to the different crushing efficiencies for analysis of noble gas and halogens.

$1.2–2.0 \times 10^{-12}$ cm^3 STP g^{-1}, respectively). Arsenopyrite 1 is characterized by significantly lower concentrations of these nuclides in the trapped hydrothermal fluids ($69–78 \times 10^{-12}$, $4.1–4.2 \times 10^{-12}$ and $0.5–0.6 \times 10^{-12}$ cm^3 STP g^{-1}, respectively), compared to the other two minerals.

Noble gas isotopic ratios are as follows: ^{3}He/^{4}He ratios are ~0.08–0.2 Ra for quartz, 0.16–0.23 Ra for arsenopyrite 1, and ~0.024 Ra for scheelite (^{3}He/^{4}He ratios of samples are given in units of the atmospheric ^{3}He/^{4}He ratio $Ra = 1.4 \times 10^{-6}$); ^{40}Ar/^{36}Ar ratios are between 304 and 498 for the studied minerals, whereas all other ratios (i.e., ^{38}Ar/^{36}Ar and the Ne, Kr and Xe isotope ratios) are atmospheric within error limits and are therefore not shown in Table 1. The ratio ^{3}He/^{36}Ar shows the strongest variability and is $\sim 0.5–0.9 \times 10^{-6}$ for quartz (with uncertainties up to 120%), $\sim 9 \times 10^{-6}$ for scheelite and $0.7–1.2 \times 10^{-4}$ for arsenopyrite 1. The F^4He values (defined as $F^4\text{He} = (^4\text{He}/^{36}\text{Ar})_{sample}/(^4\text{He}/^{36}\text{Ar})_{air}$; e.g., Kendrick et al., 2001), which provide a good estimate for the atmospheric He contribution to the sample fluid, are 13–40 for quartz, ~1500 for scheelite and ~1900 to ~2200 for arsenopyrite 1. Data from trace element analysis of the host minerals are summarized in Table 2. They are used for estimation of concentration and composition of radiogenic He produced *in situ* in the studied vein mineral samples (see below, Section 4.7).

4.2. Carbon isotope data of hydrothermal ore fluids and carbonate

Carbon isotopes were analyzed in fluids trapped in five quartz samples (Table 1). The δ^{13}C values for these fluids range from −2.1‰ to −5.3‰ (vs. PDB). It appears that with increased CO_2/CH_4 ratios, as determined by fluid inclusion studies (e.g., Graupner et al., 2001), the carbon isotopes show significantly lower values. Carbonate intergrown with vein quartz in one of the studied samples yields an even lower δ^{13}C value of −8.9‰.

4.3. Halogen geochemistry of hydrothermal ore fluids

Halogen contents for quartz and scheelite are also listed in Table 1. Only those samples are listed in Table 1 for which noble gas and/or carbon isotope data were determined in this study in addition to the halogen data. The Cl concentrations range from ~200 to ~1500 mM/l and those of Br are between ~0.2 and ~1.8 mM/l (18 samples). The log(Br/Cl) values range from −2.64 to −3.23, with just one sample below −3.00. The Cl and Br concentrations are predominantly in the same range as previously published data for a different sample set from Muruntau and Myutenbai (Cl: ~340–2100 mM/l, Br: 0.2–2.3 mM/l, excluding the samples from early horizontal quartz veins; Graupner et al., 2001). Nevertheless, the Br/Cl ratios in the present study are, on average, slightly higher than those from Graupner et al. (2001).

The ^{40}Ar*/Cl (^{40}Ar* is "excess ^{40}Ar", defined as $^{40}\text{Ar}_{measured} - {}^{36}\text{Ar}_{measured} \times (^{40}\text{Ar}/^{36}\text{Ar})_{air}$) and Cl/^{36}Ar ratios calculated from the combined noble gas and halogen data are available for fluids trapped in quartz and scheelite only. The ^{40}Ar*/Cl ratios range from $\sim 5 \times 10^{-6}$ to $\sim 11 \times 10^{-6}$ for quartz; a higher value was calculated for scheelite ($\sim 21 \times 10^{-6}$). The Cl/^{36}Ar ratios are between $\sim 2 \times 10^6$ and $\sim 5 \times 10^6$ for both minerals with the value for scheelite located at the high end of this range. However, it must be kept in mind that these values are only accurate to a factor of ~2, as the crushing efficiencies are <100% and may be different for noble gases and halogens.

4.4. Contribution of atmospheric noble gas components

In Fig. 4, the ^{3}He/^{36}Ar, ^{20}Ne/^{36}Ar, ^{84}Kr/^{36}Ar and ^{132}Xe/^{36}Ar ratios are plotted for all investigated minerals relative to the respective atmospheric values. The ratio ^{3}He/^{36}Ar is clearly elevated by orders of magnitude for fluids in scheelite and arsenopyrite, indicating that ^{3}He stems from a non-atmospheric source (see next section). The other ratios are elevated by factors of up to ~4. For Ar, Kr and Xe the pattern is similar to that typical for air-saturated water, whereas the Ne abundance is too high. Though the Ne excess is difficult to understand, this has been observed before in crustal fluids (e.g., Battani et al., 2000). Taking into account the atmospheric isotopic composition, it is justified to argue that the noble gases Ne, Ar, Kr and Xe trapped in the hydrothermal fluids of the

Table 2
Trace element contents (ppm) in the studied vein mineral samples from the Muruntau system

	Li	Be	Sr	La	Ce	Pr	Nd	Sm	Gd	Pb	Th	U
Scheelite 2												
MT1-EG-sch	0.03	0.079	820	47.6	144	25.7	123	47.8	56.8	3.3	0.31	3.36
Arsenopyrite 1												
78-98-EG-6-2-apy	1.2		1.7	0.24	0.36	0.04	0.19	0.04	0.05	13.6	0.14	0.037
300-98-EG-24-apy	1.1		1.4	0.61	1.07	0.11	0.46	0.09	0.06	5.4	0.03	0.064
Quartz												
300-98-EG-24-qtz	b.d.	<0.05	2.4	0.06	0.13	0.01	0.05	0.01	0.01	2.5	0.03	0.015
128-98-AEG-3	7.1	<0.05	4.0	0.22	0.38	0.04	0.16	0.04	0.03	1.7	0.03	0.012
128-98-AEG-4	1.8	<0.05	4.4	0.03	0.08	0.01	0.03	b.d.	b.d.	1.0	0.01	b.d.
78-98-EG-5-3	2.5	<0.05	3.2	0.36	0.62	0.06	0.27	0.05	0.02	0.3	0.03	0.016
78-98-EG-5-4	2.6	<0.05	4.2	0.02	b.d.	b.d.	0.02	b.d.	0.01	3.2	0.01	b.d.

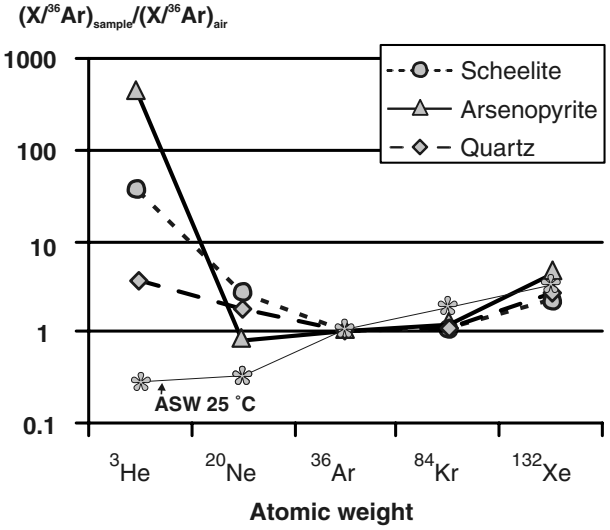

Fig. 4. Noble gas elemental ratios for quartz, arsenopyrite 1 and scheelite plotted as $(X/^{36}Ar)_{sample}/(X/^{36}Ar)_{air}$. For quartz and arsenopyrite 1 the averages of all analyzed samples were used. The element distribution for atmospheric noble gases dissolved in water at 25 °C (ASW, air-saturated water) is shown with the flower symbol. For details see text.

studied samples are dominated by gases of atmospheric origin, except for excesses of the radiogenic isotope ^{40}Ar.

4.5. Origin of helium in the trapped fluid

Helium in fluid inclusions of minerals may be composed of two components: (i) a component transferred to the studied host mineral by fluids of uncertain origin and (ii) an *in situ* produced radiogenic component. The latter factor will be discussed in more detail in Section 4.7. The data presented here yield constraints on the possible sources of He in the studied fluids based on several lines of evidence: (i) The measured $^3He/^4He$ ratios for quartz and arsenopyrite 1 are distinctly higher than the crustal values (0.01–0.05 Ra; e.g., Ballentine and Burnard, 2002) but significantly lower than atmospheric (1 Ra) and sub-continental mantle ratios (4.7–6.1 Ra; e.g., Dunai and Baur, 1995). The value for scheelite is in the crustal range; however, this value is probably strongly modified by post-entrapment radiogenic He production (see Section 4.7). (ii) The $^4He/^{20}Ne$ ratios determined for the arsenopyrite 1 (~750 to ~810) and also for the scheelite (~190) are three orders of magnitude above those of air (0.319) and air-saturated water (0.274 at 25 °C). Applying a correction for air-derived contributions to the He isotopic composition (e.g., Craig et al., 1978), the elevated $^3He/^4He$ ratios of the arsenopyrite remain nearly unchanged. Therefore, the total He in the Muruntau fluids as sampled by the arsenopyrite cannot simply be a mixture of fluids from crustal and atmospheric sources. For quartz, the $^4He/^{20}Ne$ ratios are between ~2 and ~7 and, therefore, the corrected $^3He/^4He$ ratios (0.03–0.13 Ra) partly overlap with the crustal range. (iii) The Li concentrations for our samples (Table 2) are far too low (well below 100 ppm Li; Ballentine et al., 2002) to account for significant *in situ* production of ^3He, and are not high enough to raise the $^3He/^4He$ ratio to the values observed in the crushing extractions for arsenopyrite (i.e., by a factor of ~10, cf. Mamyrin and Tolstikhin, 1984; Marty et al., 1993). Another source of ^3He is needed. (iv) The studied sample material is almost exclusively derived from underground workings (6 out of 8 samples) and, therefore, a cosmogenic production of helium (by cosmic-ray irradiation at the Earth's surface; e.g., Niedermann, 2002) can be excluded for these samples. These arguments indicate that the $^3He/^4He$ ratios in the measured fluids of up to 0.23 Ra, which are clearly increased relative to crustal values, can only be derived from an input of mantle-derived He into the mineralizing hydrothermal fluid system at Muruntau, because the mantle is the only ^3He-enriched endogenic source known so far (e.g., Burnard et al., 1999) and exogenic or radiogenic sources can be excluded.

4.6. Fluid-wall rock interaction in the crust

When assuming a high-temperature "pure" ascending (juvenile) fluid involved in the Muruntau hydrothermal system (i.e., before mixing with surface-derived meteoric fluids), the related $^3He/^4He$ ratio of such a fluid can be estimated at $\leqslant$0.5 Ra for the quartz and arsenopyrite samples using the method proposed by Burnard et al. (1997, 1999). The scheelite sample was excluded for this estimation because of its much lower $^3He/^4He$ ratio compared to the other minerals. This relatively lower ratio for scheelite may be explained by the relatively high U concentration in the host mineral (radiogenic *in situ* production of ^4He; see Section 4.7 below).

The above estimated $^3He/^4He$ ratio of the "pure" ascending fluid is significantly lower than values for potential sources in the sub-continental mantle (4.7–6.1 Ra; e.g., Dunai and Baur, 1995). Burnard et al. (1999) inferred for a similar case (the Ailaoshan gold deposits of China) that the radiogenic noble gases responsible for these lowered $^3He/^4He$ ratios were most likely introduced into the fluid from the crust before mixing with air-saturated water. Assuming a mantle $^3He/^4He$ of ~6 Ra (e.g., Dunai and Baur, 1995), the percentage of crustal ^4He in the ascending (^3He-rich) fluid can be estimated (see Burnard et al., 1999, for details). For the mineral with the highest $^4He/^{20}Ne$ ratios found in this study (i.e., the mineral with the lowest atmospheric contribution), which is the arsenopyrite 1, the contribution of crustal ^4He is calculated at ~95% to ~97%.

Another possible explanation for the low $^3He/^4He$ ratios in the fluids is the introduction of radiogenic helium into a parent magma during magmatic assimilation of crustal material or a "magma aging" process, where ^4He is produced in a long-lived magma chamber by decay of U-series elements prior to exsolution of the later trapped fluid (e.g., Simmons et al., 1987). These authors considered that a value of ~3 Ra may develop in some evolved magmatic bodies; however, this value strongly depends on the age

of the intrusion, its U content and the U/He ratio. The influence of such a scenario on the contribution of crustal ^{4}He to the Muruntau hydrothermal system cannot be calculated in detail due to the lack of information regarding the respective magma chamber, but it will not change the observed trend.

4.7. Estimation of post-entrapment radiogenic He production

To further constrain characterization of the He isotopic composition of the fluids trapped in the vein samples, we estimated the concentration and composition of radiogenic He produced *in situ*. For calculation of the radiogenic ^{3}He/^{4}He ratios the equation (7.4) of Mamyrin and Tolstikhin (1984) was used:

$$\left(\frac{^3\mathrm{He}}{^4\mathrm{He}}\right)_{\mathrm{calc}} = n_f \left\{\frac{\sum_k q_k S_k N_k}{\sum_i S_i N_i}\right\} P_{t0} \left\{\frac{\sigma_{\mathrm{Li}} N_{\mathrm{Li}}}{\sum_i \sigma_i N_i}\right\} \quad (1)$$

The values for the neutron yields in (α, n) reactions (q_i), the cross-sections for neutron capture (σ_i), and for the relative brake capacities (S_i) of each element i relevant for the quartz samples were taken from the same authors. $n_f \approx 1.15$ is the neutron yield from spontaneous fission of ^{238}U; N_i is the number of atoms of each element i per gram of rock; $P_{t0} \approx 0.8$ is the probability for a neutron to reach epithermal energy (Mamyrin and Tolstikhin, 1984, and citations therein). The trace element compositions of the samples used for calculation of the radiogenic ^{3}He/^{4}He ratios are listed in Table 2.

For the vein quartz, the calculated radiogenic ^{3}He/^{4}He ratios range from ~2 to 8×10^{-9}, except for sample 300-98-EG-24, which has a very low value of 3.5×10^{-10} due to a Li content that is an order of magnitude lower than the values for the other samples, at similar U and Th concentrations. Radiogenic ^{3}He/^{4}He ratios for the arsenopyrite 1 and scheelite samples were estimated using the values of Matsunobu et al. (1991) for the q_i of Ca, Fe and S. The aforementioned authors estimated the neutron yields for unmeasured elements using the evaporation theory. Due to the high Coulomb barrier, there is only a very low probability of (α, n) excitation from radioisotopes for heavy nuclides such as W and As. Thus, we set the value for the neutron yields for these elements to zero in our calculations. The σ_i for W and As used in this study are taken from Holden (1990). The resulting radiogenic ^{3}He/^{4}He ratios are $\sim 1.5 \times 10^{-12}$ for arsenopyrite 1 and $\sim 3.3 \times 10^{-13}$ for scheelite. Therefore, the ^{3}He/^{4}He ratios from the *in situ* production are between one and five orders of magnitude lower than crustal values in all Muruntau samples.

The amount of *in situ* radiogenic production of ^{4}He in the minerals can be estimated based on the U and Th concentrations listed in Table 2 and an age of the Muruntau deposit of ~275 Ma (e.g., Kostitsyn, 1996; Kempe et al., 2001a). ^{4}He is also produced by α-decay of ^{147}Sm. However, due to the long half-life and the production of only one α-particle per decay, the contribution of ^{147}Sm to ^{4}He production can safely be neglected relative to those of U and Th (6–8 α-particles per decay), as it is <2% even for the Sm-rich scheelite and much less for all the other samples. The expected radiogenic ^{4}He concentrations of $3.5–7.7 \times 10^{-7}$ cm^3 STP g^{-1} for quartz, $2.3–2.4 \times 10^{-6}$ cm^3 STP g^{-1} for arsenopyrite 1, and 1.2×10^{-4} cm^3 STP g^{-1} for scheelite are higher by factors of 50–600 than the actually measured ^{4}He concentrations in the fluid inclusions. However, it has to be taken into consideration that probably only a small fraction of the radiogenic helium produced in the host minerals has been transferred into the trapped fluids by diffusion. Some radiogenic helium from the host mineral lattice may also have been released during crushing of the sample, but probably the radiogenic He produced *in situ* in the host minerals does not provide a major contribution to the gas composition in the fluid inclusions, except perhaps for the U-rich scheelite.

4.8. Estimation of the percentage of mantle-derived helium at Muruntau

All measured ^{3}He/^{4}He ratios were corrected for atmosphere-derived contributions by using the observed air-derived ^{20}Ne concentration (Craig et al., 1978). Using the crustal ^{3}He/^{4}He ratio, the percentage of mantle-derived ^{4}He can then be calculated according to the crust–mantle mixing model (e.g., Ballentine et al., 2002) expressed as:

$$\mathrm{He}_{\mathrm{mantle}}(\%) = \left\{\left(\frac{^3\mathrm{He}}{^4\mathrm{He}}\right)_{\mathrm{sample}} - \left(\frac{^3\mathrm{He}}{^4\mathrm{He}}\right)_{\mathrm{crust}}\right\} / \left\{\left(\frac{^3\mathrm{He}}{^4\mathrm{He}}\right)_{\mathrm{mantle}} - \left(\frac{^3\mathrm{He}}{^4\mathrm{He}}\right)_{\mathrm{crust}}\right\} * 100 \quad (2)$$

Assuming a ^{3}He/^{4}He ratio of ~6.1 Ra for a local sub-continental lithospheric mantle source (e.g., Dunai and Baur, 1995), the calculated fractions of mantle-derived ^{4}He for Muruntau are ⩽2.1% for quartz, 2.5–3.6% for arsenopyrite 1, and 0.2% for scheelite. The values become slightly higher (⩽2.7% for quartz, 3.2–4.7% for arsenopyrite 1 and 0.3% for scheelite) when using a value of ~4.7 Ra for the mantle source. Even in the unlikely case that the fluid would be dominated by *in situ* produced radiogenic helium instead of crustal helium, the fractions of mantle-derived ^{4}He would only be increased to a maximum of 2.8% for the quartz, 4.9% for the arsenopyrite 1, and 0.5% for the scheelite, as estimated by using the radiogenic ^{3}He/^{4}He ratios calculated for the respective samples as discussed in Section 4.7.

5. Discussion

5.1. Fluid characteristics of different vein minerals

The different host minerals analyzed in this study are characterized by a significant variability in the noble gas isotopic ratios of the trapped fluids. This is best explained

in two different ways: (i) entrapment of a fluid with variable contributions from different sources into the different samples, or (ii) modification of the fluid after entrapment. As indicated by previous studies and in agreement with petrographic observations, scheelite and arsenopyrite are more resistant to recrystallization and, therefore, against alteration of trapped early fluids than the hydrothermal quartz. Therefore, it seems likely that all intimately intergrown minerals (e.g., cogenetic vein quartz and arsenopyrite 1) trapped a similar fluid, but the fluid trapped in quartz was overprinted by later, lower-temperature circulating fluids. A direct comparison of the noble gas (He) isotopic ratios appears only useful for quartz and arsenopyrite 1, because scheelite has a significantly higher radiogenic (*in situ*) production of helium due to its elevated U concentration (Table 2; cf. Section 4.7).

All minerals studied in this project are intergrown with native Au: (i) arsenopyrite 1, scheelite and quartz with Ag-poor Au 1, and (ii) intensely recrystallized quartz with Au 1 and probably remobilized Au 2 (Graupner et al., 2005). In the $^{40}Ar/^{36}Ar$ vs. $^{3}He/^{36}Ar$ plot an increasing influence of a meteoric fluid component can be observed in the sequence arsenopyrite, scheelite, and quartz (Fig. 5). From the fact that Au 1 was probably formed cogenetically with arsenopyrite 1 (Au 1 is enclosed by and influenced in growth by arsenopyrite 1; Fig. 3 and vice versa; Graupner et al., 2005), it is inferred that the primary ore-forming fluid responsible for formation of Au 1 underwent only low contamination by a meteoric component ($^{4}He/^{20}Ne$: ~750–810; $F^{4}He$ values: ~1900–2200 for arsenopyrite 1). Increased circulation of secondary fluids occurred subsequently to the formation of the studied vein minerals and is documented by secondary, low temperature fluid inclusions in quartz (e.g., Graupner et al., 2001). The arsenopyrite apparently remained sealed during these late events, whereas the quartz trapped significant amounts of late, low-temperature fluids, which modified the bulk noble gas signature of the samples.

Halogen data (Br/Cl ratios) for quartz and scheelite are not significantly different; the data for the scheelite (Br/Cl: 0.0013–0.0019) cover nearly the total range found for quartz (data from this study and Graupner et al., 2001). Halogen data for the arsenopyrite 1 are not available at present.

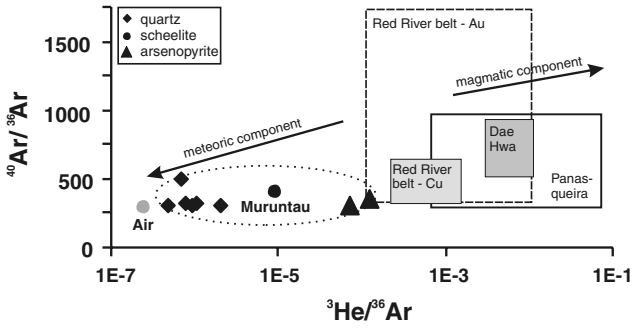

Fig. 5. $^{40}Ar/^{36}Ar$ vs. $^{3}He/^{36}Ar$ for Muruntau fluid inclusions in the host minerals quartz, arsenopyrite 1 and scheelite from ore veins. Data for Red River Au and Cu deposits are from Hu et al. (2004), for the Dae Hwa W–Mo mineralization from Stuart et al. (1995) and for the Panasqueira W deposit from Burnard and Polya (2004).

5.2. Evolution of the Muruntau system

Carbonates within metasedimentary rocks of the "Variegated Besapan" have the following stable isotope characteristics: $\delta^{13}C$: −8.9‰ to −19.7‰; $\delta^{18}O$: +16.0‰ to +11.5‰ (Kryazhev, 2002). These data suggest an origin of the carbon in the carbonates from the surrounding wall rocks by destruction of organic matter without a significant input of CO_2 from another source. Metamorphic rock reactions in the metasedimentary rocks are considered as the main source of fluids present during deformation of the earliest vein-type formations at Muruntau, the horizontal quartz veins, as indicated by halogen ratios (Br/Cl vs. Cl) for fluids trapped in inclusions in flat vein quartz (Graupner et al., 2001) and REE characteristics of associated scheelite (scheelite 1 of Kempe et al., 2001a).

The noble gas isotopic ratios ($^{3}He/^{4}He$; $^{4}He/^{20}Ne$) of fluids trapped in minerals (arsenopyrite 1, scheelite) from Au-mineralized vein types formed during the main stage of hydrothermal activity at Muruntau provide evidence for a contribution from a mantle-derived source to the ascending fluids responsible for formation of the economic Au-mineralization at Muruntau. The data indicate that the trapped hydrothermal fluids always contain He contributions from different sources; however, the amounts vary strongly between the considered sources as well as between the studied minerals.

The mantle fluid He component is below 5% for all studied minerals. The highest contribution to the total He, with >95%, comes from crustal source(s). These data fit very well the homogeneous initial ratios defined for Sr and Nd of the strongly altered metasedimentary host rocks at Muruntau (Kostitsyn, 1996; Kempe et al., 2002), as well as the clearly crustal Sr and Nd isotope signatures found for scheelite, which is intergrown with native Au in the high-grade mineralized central ore veins (Kostitsyn, 1996; Kempe et al., 2001a). All these data confirm very intense interactions between the ascending hydrothermal ore fluids and the crustal rocks within the Muruntau ore field, as indicated by the $^{3}He/^{4}He$ ratios. Variable fractions of the noble gases Ar and He, as well as the dominant portions of the Ne, Kr and Xe in the hydrothermal fluids, come from meteoric fluids (Fig. 5; see above).

Using these data, two genetic models for locations of initial fluid–rock interaction processes can be considered. Mushkin and Jaroslavsky (1976) and Babaev (1983) discussed zones of metamorphic alteration in the lower crust (formation of eclogites), which were stimulated by an input of mantle fluids, as a source of gold introduced into the ore systems. Their model is based on the investigation of xenoliths from dikes of the Southern Tien Shan complex. On the other hand, the distinctly crustal signatures in the noble gas data also support intense interactions of the ascending

fluids with the ore-hosting and underlying metasedimentary packages. Therefore, a possible contribution of originally finely disseminated gold from stratigraphic gold-bearing (carbonaceous) packages in the Besapan (regional geochemical anomalies) also has to be considered (e.g., Garkovets, 1973; Prozenko, 1987). For example, Wilde (2005) found Au concentrations of <1–2 ppb for unmineralized carbonaceous metapelites from the environs of the Muruntau mine.

The involvement of mantle-derived sources during the main hydrothermal stage within the Muruntau Au system is further supported by geological and geochemical indications. The most remarkable aspect is the presence of lamprophyric dikes occurring in similar structural positions as Au-mineralized vein structures at Muruntau (cf. Kempe et al., 1997). The dike belts north and south of the deposit, which contain a significant amount of lamprophyres, have a similar trend (E-W-trend; A.K. Voronkov (personal communication) in Kostitsyn, 1996) as the faults that provide the space for the large auriferous quartz bodies in the deposit (Obraztsov, 2001). The intrusion ages of these dikes have been constrained at 273 ± 3 Ma using Rb–Sr dating (Kostitsyn, 1996). This age—if not reflecting later alteration—is, within error, indistinguishable from that of the economic hydrothermal Au mineralization at Muruntau. Furthermore, the geochemical compositions of the ore and the near-ore alteration assemblages, which contain Te, Se, Pt and platinum-group elements as well as Hg (Ermolaev, 1995; Golovanov et al., 1998a), may suggest contributions to the ore components from the mantle. Wilde (2005) reports up to 100 ppb Pt and 132 ppb Pd for high-grade dump ore (metapelitic rocks and so-called ''metasomatites'') from Muruntau.

The presence of a zone of increased heat flow from the mantle in Central Asia in general (in the Karakum-Kyzylkum-Kuraminsk-Issykkul mega-zone; Borisov, 1988), as indicated by geothermal studies by J.N. Suev (in Golovanov et al., 1998a), and an abnormal heat flow gradient in the central parts of the Muruntau system were interpreted by several authors (e.g., Kremenetsky and Minzer, 1995) to result from the formation of an asthenospheric plume during the collisional stage of the Hercynian collision in the western Tien Shan (e.g., Berger et al., 1994). However, the $^3He/^4He$ isotopic ratios of this study (⩽0.23 Ra) are too low to support a direct plume-related contribution to the He in the hydrothermal fluids at Muruntau, as assumed in the so-called ''fluid-magmatic model'' of Kremenetsky and Minzer (1995). $^3He/^4He$ ratios for plume-related fluids can be as high as >30 Ra (Graham, 2002).

Another model which has been put forward to explain an input of fluids from a mantle source into the Muruntau system as part of the Kyzylkum ore province is the ''subduction-hydrothermal model'' of Savchuk and Mukhin (1993). These authors assume an origin of fluids responsible for ore formation in this ore province (the so-called Kyzylkum accretionary prism) from the melting of a subducted oceanic plate and a subsequent separation of fluids enriched in gold, at depth. The assumed Hercynian age for a suture zone north of Muruntau (Kotov and Poritskaya, 1992; Berger et al., 1994) justifies consideration of this model. $^3He/^4He$ ratios of arc-related volcanism, even at segments with significant volumes of subducting sediments, often fall into the MORB-He isotope range (8 ± 1 Ra; Hilton et al., 2002), suggesting little or no slab influence. The helium in the majority of arcs is predominantly of mantle derivation, and presumably derived from the mantle wedge (e.g., Hilton et al., 2002). If such a scenario was also valid for the studied area, then the signature of radiogenic helium was most probably acquired during travelling of the fluids through the metasedimentary units. Another possibility of producing $^3He/^4He$ ratios <1 Ra in an arc system is the subduction of crust of continental affinity, as shown by Hilton et al. (1992) for the east Sunda/Banda arcs in Indonesia.

The Br/Cl ratios of the fluids trapped within the steeply dipping vein structures at Muruntau are in agreement with the presence of a juvenile fluid component at Muruntau as suggested by the noble gas isotopic data. In addition, they indicate variable contributions from metamorphic and deep-seated sources to the ore-bearing fluids circulating during formation of the economic Au mineralization in different parts of the Muruntau/Myutenbai system. The indicated elevated concentrations of juvenile fluids in quartz of steeply dipping veins from the Myutenbai system are consistent with slightly higher temperatures of homogenization (T_h) for primary or pseudosecondary fluid inclusions from the Myutenbai location compared to similar veins from Muruntau (Graupner et al., 2001). These data may be explained by an expected more efficient fluid and heat transfer from deep sources in this area, which is located close to both, the northwestern margin of a geophysically indicated magmatic body (see Revyakin in Shayakubov et al., 1998) and also the Murun granite, compared to the more ''distal'' Muruntau system.

Stable isotopic data ($\delta^{13}C$) for vein quartz and carbonate from the main stage of hydrothermal activity indicate a significant input of fluids from a juvenile source into the Au-bearing stockwork and high-grade auriferous central veins during the main stage of high temperature wall rock alteration (biotitization and K-feldspatization) and initial ore vein formation in the Muruntau system. Interestingly, there is a good correlation of the $\delta^{13}C$ values with the CO_2/CH_4 ratios of the trapped fluids. Quartz samples bearing Au 1 only and having low fluid CO_2/CH_4 ratios (3.7–4.1) show $\delta^{13}C$ values of the fluid between −2.1‰ and −3.4‰. On the other hand, samples containing Au 1 and secondary Au 2, as well as increased fluid CO_2/CH_4 values (~9.0) yield $\delta^{13}C$ values of the fluid between −4.3‰ and −5.4‰. The range of $\delta^{13}C$ for mantle fluids is −5 ± 2‰ (Deines, 1980). Thus, it may be suggested that a juvenile contribution to the fluids was obtained. Carbon isotope data for carbonates of quartz–potash feldspar altered metasediments associated with the main ore stage indicate

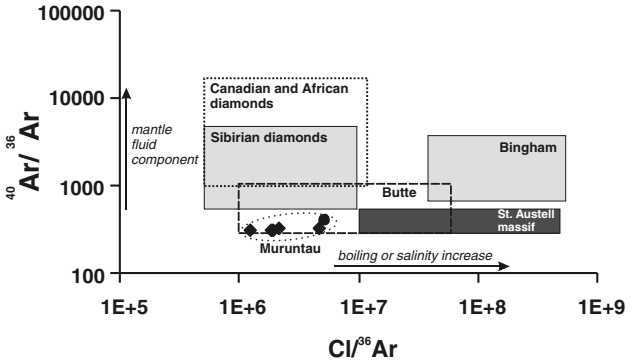

Fig. 6. $^{40}Ar/^{36}Ar$ vs. $Cl/^{36}Ar$ for fluid inclusions in quartz and scheelite from Muruntau veins. Data for Butte, Bingham, and St. Austell fluid inclusions are from Irwin and Roedder (1995). Fields for fluids from Canadian and African diamond, as well as from Sibirian diamond occurrences were constructed using results of Johnson et al. (2000) and Burgess et al. (2002), respectively. Symbols are as in Fig. 5.

disequilibrium conditions between the carbonates and the organic material in the surrounding rocks (Kryazhev, 2002). This author interprets this observation in terms of a possible input of CO_2-bearing fluids from a juvenile source. C and O isotope ratios of vein carbonate formed in the final stages of the main hydrothermal event at Muruntau also show values consistent with such a scenario ($\delta^{13}C$: −4.9‰ to −8.5‰; $\delta^{18}O$: 12.5–18.2‰; Kryazhev, 2002).

For the late, post-economic gold mineralization stages of the evolution of the Muruntau system, including retrograde alteration of the wall rocks and sub-economic Au–Ag vein formation, an input of descending fluids from the overlying calcareous packages or from an adjacent major rift has been proposed by several authors (e.g., Wilde et al., 2001; Kryazhev, 2002). Wilde et al. (2001) linked these reduced sulfur-rich fluids with 245 and 220 Ma $^{40}Ar/^{39}Ar$ ages for hydrothermal sericite from stockpile ores at Muruntau.

5.3. Comparison with other systems

$^{40}Ar/^{36}Ar$ and $^{40}Ar^*/Cl$ ratios for Muruntau fluids (Figs. 6 and 7) are significantly lower than those for mantle-derived fluids in Sibirian, Canadian and African diamonds (Burgess et al., 2002; Johnson et al., 2000). Based on a comparison with these data, it is evident that argon is dominated by an atmospheric component in the Muruntau fluids. Even the highest $^{40}Ar/^{36}Ar$ fluid ratios in scheelite are probably not mantle-derived (as is valid for the diamonds), but of crustal origin (radiogenic), like most of the ^{4}He in the scheelite.

In the $^{40}Ar/^{36}Ar$ vs. $Cl/^{36}Ar$ plot (Fig. 6) the data from Muruntau are compared with other typical ore systems. The $Cl/^{36}Ar$ ratios for Muruntau quartz and scheelite plot in a similar field as the data for the Butte system, which is dominated by meteoric waters (e.g., Shephard and Taylor, 1974; Irwin and Roedder, 1995). The $Cl/^{36}Ar$ ratios for both host minerals are clearly lower than those for typical juvenile fluid-dominated systems (e.g., at Bingham and St. Austell; Irwin and Roedder, 1995). However, the data for the arsenopyrite 1 from Muruntau, for which Cl data are unfortunately not available, are expected to plot at ratios much closer to those of St. Austell. A significantly smaller meteoric component for the arsenopyrite 1 samples, compared to quartz and scheelite, is indicated by their higher $^3He/^{36}Ar$ ratios (Fig. 5). Further support for a limited influence of meteoric fluids during arsenopyrite 1 formation comes from the high F^4He values for the fluid in this mineral (~1900 to ~2200). The data for quartz samples which show evidence for fluid phase separation (Graupner et al., 2001) are located mostly at the high end of the range for $Cl/^{36}Ar$ for the Muruntau samples. This is interpreted as the result of fractionation of noble gases from Cl during fluid phase separation, as also suggested by Kendrick et al. (2001) for Cu-porphyry mineralizing fluids. In the $^{40}Ar^*/Cl$ vs. Br/Cl plot (Fig. 7) most Muruntau data ($^{40}Ar^*/Cl$: $4.6–21 \times 10^{-6}$) plot above the $^{40}Ar^*/Cl$ ratios typical of crustal fluids ($^{40}Ar^*/Cl$: $0.6–5.0 \times 10^{-6}$; Turner and Bannon, 1992). Ballentine et al. (2002) interpreted such elevated ratios as being due to the thermal release of excess ^{40}Ar from the host mineral during metamorphic reactions. In this plot the field for the Muruntau data significantly overlaps with those for trapped fluids in samples from the Bingham system and also from Ascension Island, which are both interpreted to have an unmodified, magmatic origin (Irwin and Roedder, 1995). The Br/Cl ratios at Muruntau are higher than those of the St. Austell granite and overlap only somewhat at

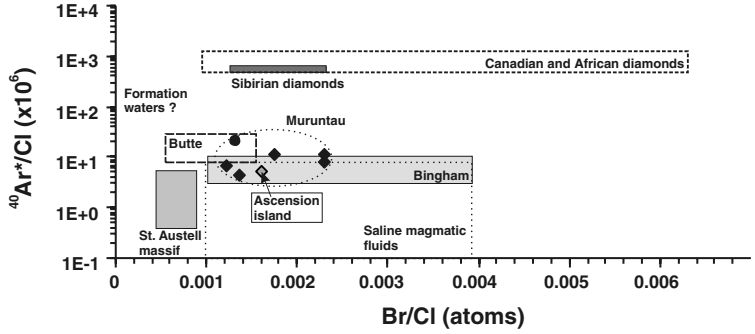

Fig. 7. $^{40}Ar^*/Cl$ vs. Br/Cl ratios for fluid inclusions in quartz and scheelite from Muruntau veins. Data sources and symbols are as in Figs. 5 and 6.

the low end of their range with the Butte data (Irwin and Roedder, 1995). These authors suggested that the juvenile fluids at St. Austell were mixed with salts from metasedimentary packages having lower Br/Cl ratios.

6. Summary and conclusions

Our new noble gas isotope, halogen and carbon isotope data, as well as published Rb–Sr and Sm–Nd isotope (Kostitsyn, 1996; Kempe et al., 2001a), REE (Kempe et al., 2001a,b), and fluid inclusion data (Graupner et al., 2001, 2005; Wilde et al., 2001) strongly suggest that diverse sources were involved in the formation of the large hydrothermal Muruntau gold system. On the one hand, crustal signatures were obtained by the fluids during very intense and extended fluid-wall rock interaction. On the other hand, the noble gas data discussed here along with halogen and REE data indicate that there was also an input from external, deep-seated (mantle and possibly lower crust) sources. Furthermore, significant fractionation also occurred during evolution of the ore-forming system, as indicated by fluid inclusion data (phase separation) and REE characteristics of monazite and scheelite. At present, it is therefore difficult to constrain the source(s) of the gold; remobilization from the wall rocks, supply from the lower crust, granite-related fluid sources, as well as an input from the mantle, all have to be considered. Some of these possibilities may be excluded when the absolute and relative time sequences are better constrained and when the chemical peculiarities of these processes are considered. At present, we prefer an external input from a lower crustal and/or mantle source to be a dominant factor in formation of the large Muruntau gold deposit.

Acknowledgments

The authors wish to express their gratitude to Navoi Mining and Metallurgical Complex, Zarafshan Central Mine Board, Uzbekistan, who allowed us to conduct investigations on their property. We particularly thank Prof. A.A. Kremenetsky, Dr. I.M. Golovanov and N.P. Snitka for their support during field work. We thank E. Schnabel for performing the noble gas analyses and Dr. K. Hahne, H. Rothe and S. Tonn for determining the trace element compositions. Prof. D. Wolf is thanked for his continuous support of the project. Prof. E.T.C. Spooner and Dr. C.J. Bray from the F. Gordon Smith Fluid Incl. Lab., Department of Geology, University of Toronto, are greatly acknowledged for joint analytical work and fruitful discussions. Technical assistance by R. Hoffbauer from the University of Bonn is much appreciated. We thank the Associate Editor Dr. U. Reimold and two anonymous reviewers for helpful comments that greatly improved the manuscript.

Associate editor: W. Uwe Reimold

References

Arifulov, Tsh.Kh., 1976. Mineralogy and genesis of veinlet zones with gold-sulfide mineralization in the Kyzylkum. *Uzbekskii Geologitsheski Shurnal* **5**, 54–61 (in Russian).

Babaev, K.L., 1983. Genesis of gold deposits (using Central Asia as an example). In: *Recent questions concerning the geology, mineralogy and geochemistry of gold and silver in Central Asia*. SAIGIMS, Tashkent, pp. 11–26 (in Russian).

Ballentine, C.J., Burnard, P.G., 2002. Production, release and transport of noble gases in the continental crust. In: Porcelli et al. (Eds.), *Noble gases in geochemistry and cosmochemistry*. Reviews in Mineral. and Geochem. 47, The Mineralogical Society of America, Washington, pp. 481–538.

Ballentine, C.J., Burgess, R., Marty, B., 2002. Tracing fluid origin, transport and interaction in the crust. In: Porcelli et al. (Eds.) *Noble gases in geochemistry and cosmochemistry*. Reviews in Mineral. and Geochem. 47, The Mineralogical Society of America, Washington, pp. 539–608.

Battani, A., Sarda, P., Prinzhofer, A., 2000. Basin scale natural gas source, migration and trapping traced by noble gases and major elements: the Pakistan Indus basin. *Earth Planet. Sci. Lett.* **181**, 229–249.

Bel'kova, L.N., Ognev, V.N., 1970. Age and origin of gold mineralization of the Muruntau. *Dokl. Akad. Nauk SSSR* **197**, 100–102.

Berger, B.R., Drew, L.J., Goldfarb, R.J., Snee, L.W., 1994. An epoch of gold riches: the late Paleozoic in Uzbekistan, Central Asia. *SEG Newslett.* **16**, 1–11.

Borisov, S.O., 1988. *Thermodynamic conditions at depth and dynamics of the earth crust in Central Asia*. FAN, Tashkent, 93 p. (in Russian).

Bray, C.J., Spooner, E.T.C., Thomas, A.V., 1991. Fluid inclusion volatile analysis by heated crushing, on line gas chromatography; applications to Archean fluids. *J. Geoch. Expl.* **42**, 167–193.

Bukharin, A.K., Maslennikova, I.A., Zhuravleva, I.T., Mambetov, A.M., 1984. The age of Taskazgan and Besapan suits (Lower Paleozoic) in the Kyzyl Kum and similar rocks in the Nuratau. *Byull. Mosk. Ova. Ispy. Prir., Otd Geol* **59**, 57–68 (in Russian).

Burgess, R., Layzelle, E., Turner, G., Harris, J.W., 2002. Constraints on the age and halogen composition of mantle fluids in Sibirian coated diamonds. *Earth Planet. Sci. Lett.* **197**, 193–203.

Burnard, P.G., Polya, D.A., 2004. Importance of mantle derived fluids during granite associated hydrothermal circulation: He and Ar isotopes of ore minerals from Panasqueira. *Geochim. Cosmochim. Acta* **68**, 1607–1615.

Burnard, P.G., Graham, D.W., Turner, G., 1997. Vesicle-specific noble gas analyses of "popping rock": implications for primordial noble gases in the earth. *Science* **276**, 568–571.

Burnard, P.G., Hu, R., Turner, G., Bi, X.W., 1999. Mantle, crustal and atmospheric noble gases in Ailaoshan gold deposit, Yunnan Province, China. *Geochim. Cosmochim. Acta* **63**, 1595–1604.

Channer, D.M.DeR., Bray, C.J., Spooner, E.T.C., 1999. Integrated cation–anion/volatile fluid inclusion analysis by gas and ion chromatography; methodology and examples. *Chem. Geol.* **154**, 59–82.

Cole, A., Seltmann, R., 2000. The role of granitoids during Variscan orogenic gold mineralization in the Tien Shan and Ural Mountain belts of Central Eurasia. *Documents du BRGM* **297**, 110–111.

Craig, H., Lupton, J.E., Horibe, Y., 1978. A mantle helium component in circum Pacific volcanic gases: Hakone, the Marianas, and Mt. Lassen. In: Alexander, E.C., Ozima, M. (Eds.), *Terrestrial Rare Gases*. Sci. Societies Press, Tokyo, pp. 3–16.

Deines, P., 1980. The carbon isotopic composition of diamonds: relationship to diamond shape, color, occurrence and vapor composition. *Geochim. Cosmochim. Acta* **44**, 943–961.

Drew, L.J., Berger, B.R., Kurbanov, N.K., 1996. Geology and structural evolution of the Muruntau gold deposit, Kyzylkum Desert, Uzbekistan. *Ore Geol. Rev.* **11**, 175–196.

Dunai, T.J., Baur, H., 1995. Helium, neon and argon systematics of the European subcontinental mantle: implications for its geochemical evolution. *Geochim. Cosmochim. Acta* **59**, 2767–2783.

Ermolaev, N.P., 1995. Platinum-group metals in terrigeneous–carbonaceous shales. *Geochem. Int.* **32**, 122–131.

Garkovets, V.G., 1973. New data concerning the origin of gold in deposits in black shales. *Zapiski Mineralogicheskogo Obshchestva Usbekistana* **31**, 25–28 (in Russian).

Golovanov, I.M., Nikolaeva, E.I., Kazhikhin, M.A., 1988. *Integrated model for the forecasting and prospecting of porphyry copper deposits.* Tashkent, Fan (in Russian).

Golovanov, I.M., Savchuk, Ju.S., Voronkov, A.K., Chorvat, V.A., Shvezov, A.D., Judalevitch, S.A., 1998a. Geology of the Muruntau ore field. In: Shayakubov, T. et al. (Eds.), *Muruntau Gold Ore Deposit.* Izdatel'stvo "FAN" Akademii nauk Respubliki Uzbekistan, Tashkent, Uzbekistan, pp. 78–164 (in Russian).

Golovanov, I.M., Protsenko, V.F., Arifulov, T.C., Dunin-Barkovskaya, E.A., 1998b. Mineral assemblages and industrial ore features. In: Shayakubov, T. et al. (Eds.), *Muruntau Gold Ore Deposit*. Izdatel'stvo "FAN" Akademii nauk Respubliki Uzbekistan, Tashkent, Uzbekistan, pp. 222–319 (in Russian).

Govindaraju, K., 1994. *Geostand. Newslett.* **18** (special issue), 158 pp.

Graham, D.W., 2002. Noble gas isotope geochemistry of Mid-Ocean Ridge and Ocean Island Basalts: characterization of mantle source reservoirs. In: Porcelli et al. (Eds.) *Noble gases in Geochemistry and Cosmochemistry.* Reviews in Mineral. and Geochem. 47, The Mineralogical Society of America, Washington, pp. 247–317.

Graupner, T., Götze, J., Kempe, U., Wolf, D., 2000. CL for characterizing quartz and trapped fluid inclusions in mesothermal quartz veins: Muruntau Au ore deposit, Uzbekistan. *Miner. Mag.* **64**, 1007–1016.

Graupner, T., Kempe, U., Spooner, E.T.C., Bray, C.J., Kremenetsky, A.A., Irmer, G., 2001. Microthermometric, laser Raman spectroscopic, and volatile/ion chromatographic analysis of hydrothermal fluids in the Paleozoic Muruntau Au-quartz vein ore field, Uzbekistan. *Econ. Geol.* **96**, 1–23.

Graupner, T., Kempe, U., Klemd, R., Schüssler, U., Spooner, E.T.C., Götze, J., Wolf, D., 2005. Two stage model for the Muruntau (Uzbekistan) high grade ore structures based on characteristics of gold, host quartz and related fluids. *N. Jb. Min. Abh.* **181/1**, 67–80.

Hilton, D.R., Hoogewerff, J.A., van Bergen, M.J., Hammerschmidt, K., 1992. Mapping magma sources in the east Sunda-Banda arcs, Indonesia: constraints from helium isotopes. *Geochim. Cosmochim. Acta* **56**, 851–859.

Hilton, D.R., Fischer, T.P., Marty, B., 2002. Noble gases and volatile recycling at subduction zones. In: Porcelli et al. (Eds.), *Noble Gases in Geochemistry and Cosmochemistry.* Reviews in Mineral. and Geochem. 47, The Mineralogical Society of America, Washington, pp. 319–362.

Holden, N.E., 1990. Tables of the isotopes. In: Lide, D.R. (Ed.), *Handbook of Chemistry and Physics*, seventy first ed., CRC Press, Boca Raton, USA, pp. 11–33 to 11–140.

Hu, R.Z., Burnard, P.G., Bi, X.W., Zhou, M.F., Pen, J.T., Su, W.C., Wu, K.X., 2004. Helium and argon isotope geochemistry of alkaline intrusion-associated gold and copper deposits along the Red River-Jinshajiang fault belt, SW China. *Chem. Geol.* **203**, 305–317.

Irwin, J.J., Roedder, E., 1995. Diverse origins of fluid inclusions at Bingham (Utah, USA), Butte (Montana, USA), St. Austell (Cornwall, UK), and Ascension Island (mid-Atlantic, UK), indicated by laser microprobe analysis of Cl, K, Br, I, Ba + Te, U, Ar, Kr, Xe. *Geochim. Cosmochim. Acta* **59**, 295–312.

Ivankin, P.F., Nasarova, N.I., 1991. Types of ore forming systems. *Geologija Rudnikh Meshdoroshdenii* **5**, 3–13 (in Russian).

Johnson, L.H., Burgess, R., Turner, G., Milledge, H.J., Harris, J.W., 2000. Noble gas and halogen geochemistry of mantle fluids: comparison of African and Canadian diamonds. *Geochim. Cosmochim. Acta* **64**, 717–732.

Kempe, U., Oberthür, T., 1997. Physical and geochemical characteristics of scheelite from gold deposits: a reconnaissance study. In: Papunen, H. (Ed.), *Mineral Deposits: Research and Exploration. Where Do They Meet?* Balkema, Rotterdam, pp. 209–212.

Kempe, U., Belyatsky, B.V., Kremenetsky, A.A., Wolf, D., Krymsky, R.S., 1997. Mantle influence on the genesis of the super-large Au deposit Muruntau (Uzbekistan): constraints from geochemistry and isotope composition of scheelites. In: Hatton, C.J. (Ed.), *Plumes, Plates and Mineralization*. University of Pretoria, Pretoria, pp. 51–52.

Kempe, U., Belyatsky, B.V., Krymsky, R.S., Kremenetsky, A.A., Ivanov, P.A., 2001a. Sm–Nd and Sr isotope systematics of scheelite from the giant Au(-W) deposit Muruntau (Uzbekistan): implications for the age and sources of Au mineralisation. *Miner. Depos.* **36**, 379–392.

Kempe, U., Graupner, T., Wolf, D., Kremenetsky, A.A., 2001b. Unusual REE fractionation and occurrence of monazite-(La, Ce) in single monazite grains from a, "Central" gold–quartz vein at Muruntau. In: Piestrzynski, A. et al. (Eds.), *Mineral Deposits at the Beginning of the 21st Century*. Balkema, Rotterdam, pp. 767–770.

Kempe, U., Graupner, T., Belyatsky, B., Köhler, S., Wolf, D., Kremenetsky, A.A., 2002. Wall rock alteration in the giant Muruntau Au deposit (Usbekistan): new constraints on the genesis of Au mineralisation. Geocongress 2002, Windhoek, Namibia, extended abstract, 3 p.

Kempe, U., Seltmann, R., Graupner, T., Wall, V.J., Matukov, D., Sergeev, S., 2004. SHRIMP U-Pb zircon dating of Hercynian granite magmatism in the Muruntau gold district (Uzbekistan). In: Khanchuk, A.I. et al. (Eds.), *Metallogeny of the Pacific Northwest: Tectonics, Magmatism and Metallogeny of Active Continental Margins (IAGOD Conference)*. Vladivostok, Dalnauka, pp. 210–213.

Kendrick, M.A., Burgess, R., Pattrick, R.A.D., Turner, G., 2001. Fluid inclusion noble gas and halogen evidence on the origin of Cu-Porphyry mineralising fluids. *Geochim. Cosmochim. Acta* **65**, 2651–2668.

Khamrabaev, I.K., Sidorova, I.P., Kustarnikova, A.A., Seiduzova, S.S., Polikarpov, A.A., 2003. The role of deep lithospheric structure in the genesis of large and superlarge ore deposits in Uzbekistan: a review. *Global Tectonics Metallogeny* **8**, 151–154.

Khokhlov, V.A., 1990. Petrology of metamorphic and metasomatic processes in the Muruntau ore field: In: *Special characteristics of the geology and mineralisation in the Southern Tien-Shan.* Tashkent, SAIGIMS, pp. 37–47 (in Russian).

Kostitsyn, Y.A., 1996. Rb–Sr isotopic study of the Muruntau deposit: magmatism, metamorphism, and mineralisation. *Geokhimiya* **34**, 1123–1138 (in Russian).

Kotov, N.V., Poritskaya, L.G., 1992. The Muruntau gold deposit: its geologic structure, metasomatic mineral associations and origin. *Int. Geol. Rev.* **34**, 77–87.

Kremenetsky, A.A., Minzer, E.F., 1995. Universal evolution of gold ore systems—key criteria for regional prognosis of economic ore systems. *Otechestv. Geologija* **5**, 19–27 (in Russian).

Kryazhev, S.G., 2002. *Isotopic-geochemical regime of the Muruntau gold deposit formation*. TsNIGRI, Moscow, 91 p. (in Russian).

Kudrin, V.S., Solov'yev, V.A., Stavinskiy, V.A., Karabdin, L.L., 1990. The gold–copper–molybdenum–tungsten ore belt of the Tien Shan. *Int. Geol. Rev.* **32**, 930–941.

Loshchinin, V.P., Chistyakov, P.A., Mansurov, M.M., Surgutanova, D.M., Min'kin, M.I., 1986. Metamorphic transformation of Ordovician-Silurian sediments in the Muruntau ore field. *Zapiski Uzbekskogo Otdeleniya Vsesoyuznogo Mineralogicheskogo Obshchestva* **39**, 153–161 (in Russian).

Mamyrin, B.A., Tolstikhin, I.N., 1984. *Helium Isotopes in Nature*. Elsevier, Amsterdam, 273 p.

Mansurov, M.M., Jergashev, S.J., Iskadshanov, B.I., Abduvakhabov, A., 1991. Development of ideas for the stratigraphy and age of pre-Mesozoic packages in the Central Kyzylkum. *Sapiski Usbekistanskovo Otdelenija Vsesojusnovo Mineralogitseskovo Obtsestva* **44**, 123–129 (in Russian).

Marty, B., Torgersen, T., Meynier, V., O'Nions, R.K., de Marsily, G., 1993. Helium isotope fluxes and groundwater ages in the Dogger aquifer, Pais Basin. *Water Resour. Res.* **29**, 1025–1035.

Matsunobu, H., Oku, T., Iljima, S., Naito, Y., Masukawa, F., Nakasima, R., 1991. *Data Book for Calculating Neutron Yields from (alpha, n) Reaction and Spontaneous Fission.* Report from Tokai Research Establishment, Japan.

Morelli, R.M., Creaser, R.A., Seltmann, R., 2004. Rhenium–osmium geochronology of arsenopyrite from the giant Muruntau Au deposit,

Uzbekistan. In: Khanchuk, A.I. et al. (Eds.), *Metallogeny of the Pacific Northwest: Tectonics, Magmatism and Metallogeny of Active Continental Margins (IAGOD Conference)*. Vladivostok, Dalnauka, pp. 510–513.

Mukhin, P.A., Savchuk, Y.S., Kolesnikov, A.V., 1988. The position of the "Muruntau lens" within the metamorphic rock unit of the Southern Tamdytau (Central Kyzylkum Desert). *Geotektonika* **2**, 64–72 (in Russian).

Mushkin, I.V., Jaroslavsky, R.I., 1974. Gold in alkali basalts and some types of inclusions from the depth of the Southern Tienshan. *Geokhimija* **7**, 1041–1044 (in Russian).

Mushkin, I.V., Jaroslavsky, R.I., 1976. Formation of eclogites in the granulite–basite layer as one of the sources of ore material (the western part of the Tienshan). In *Metasomatic Processes and Ore Formation*, Abstract of thesis, 21 p. (in Russian).

Niedermann, S., 2002. Cosmic-ray-produced noble gases in terrestrial rocks: dating tools for surface processes. In: Porcelli et al. (Eds.), *Noble Gases in Geochemistry and Cosmochemistry*. Reviews in Mineral. and Geochem. 47, The Mineralogical Society of America, Washington, pp. 731–784.

Niedermann, S., Bach, W., Erzinger, J., 1997. Noble gas evidence for a lower mantle component in MORBs from the southern East Pacific Rise: decoupling of helium and neon isotope systematics. *Geochim. Cosmochim. Acta* **61**, 2697–2715.

Obraztsov, A.I., 1999. Spatial–temporal and genetic aspects of the gold localization in ore mineralization (on example of Muruntau deposit). *Geol. Min. Res.* **3**, Tashkent, FAN AN RU's, pp. 18–21 (in Russian).

Obraztsov, A.I., 2001. Change of the ideas about the morphology and structure of Muruntau deposit and the efficiency of searching–prospecting works. *Geol. Min. Res.* **4**, Tashkent, FAN AN RU's, pp. 10–16 (in Russian).

Prozenko, V.F., 1987. Gold ore mineral genesis in packages of black shales in Western Uzbekistan. *Sapiski Usbekistan Otd. VMO* **40**, 21–30 (in Russian).

Savchuk, Ju.S., Mukhin, P.A., 1993. Evolution of ore processes in the structure of the accretionary prism of the Southern Tienshan (Kyzylkum geodynamic polygon). *Geotektonika* **6**, 63–81 (in Russian).

Shayakubov, T.Sh., Golovanov, I.M., Sakirov, A.T., Isakhodjaev, B.A., 1998. *Muruntau gold ore deposit,* Izdatel'stvo "FAN" Akademii nauk Respubliki Uzbekistan, Tashkent, Uzbekistan, 540 p. (in Russian).

Shayakubov, T., Kremenetsky, A.A., Minzer, E., Obraztsov, A., Graupner, T., 1999. The Muruntau ore field. In: Shayakubov, T. et al. (Eds.), *Au, Ag, and Cu Deposits of Uzbekistan*. GeoForschungsZentrum (GFZ) Potsdam, Germany, pp. 37–74.

Shephard, S.M.F., Taylor, H.P., 1974. Hydrogen and oxygen isotope evidence for the origins of water in the Boulder batholith and the Butte ore deposits, Montana. *Econ. Geol.* **69**, 926–946.

Simmons, S.F., Sawkins, F.J., Schlutter, D.J., 1987. Mantle derived helium in two Peruvian hydrothermal ore deposits. *Nature* **329**, 429–432.

Stuart, F.M., Burnard, P.G., Taylor, R.P., Turner, G., 1995. Resolving mantle and crustal contributions to ancient hydrothermal fluids: He–Ar isotopes in fluid inclusions from Dae Hwa W–Mo mineralization, South Korea. *Geochim. Cosmochim. Acta* **59**, 4663–4673.

Turner, G., Bannon, M.P., 1992. Argon isotope geochemistry of inclusion fluids from granite-associated mineral veins in southwest and northeast England. *Geochim. Cosmochim. Acta* **56**, 227–243.

Uspenskiy, Y.I., Aleshin, A.P., 1993. Patterns of scheelite mineralization in the Muruntau gold deposit, Uzbekistan. *Int. Geol. Rev.* **35**, 320–342.

Vasilevskiy, B.B., Koneev, R.I., Rustamov, A.I., Turesebekov, A.K., Ignatikov, E.N., Mirtalipov, D.Y., Rakhimov, R.R., 2004. New data on material composition of gold ores of Muruntau deposit. *Ores Metals* **2**, 67–79.

Voronkov, A.K., Yakovlev, V.G., Prozenko, V.F., 1983. On the energy of syngenetic–epigenetic ore formation. *Sapiski Usbekistan. Otd. VMO* **36**, 137–140 (in Russian).

Wall, V.J., Graupner, T., Yantsen, V., Seltmann, R., Hall, G.C., 2004. Muruntau, Uzbekistan: a giant thermal aureole gold (TAG) system. In: Muhling, J. et al. (Eds.), *SEG 2004 'Predictive Mineral Discovery Under Cover, Extended Abstracts'*. UWA Publ. No. 33, Perth, pp. 199–203.

Wilde, A., 2005. Descriptive ore deposit models: hydrothermal and supergene Pt and Pd deposits. In: Mungall, J.E. (Ed.), *Exploration for Deposits of Platinum-Group Elements*. Mineralogical Association of Canada, Short Course Series 35, pp. 145–161.

Wilde, A.R. Gilbert, D., 1999. Setting of the giant Muruntau gold deposit: implications for ore genesis. In: *Abstracts of the SME Annual Meeting*, Denver, Colorado, 6 p.

Wilde, A.R., Layer, P., Mernagh, T., Foster, J., 2001. The giant Muruntau gold deposit: geologic, geochronologic, and fluid inclusion constraints on ore genesis. *Econ. Geol.* **96**, 633–644.

Yakubchuk, A., Cole, A., Seltmann, R., Shatov, V., 2002. Tectonic setting, characteristics, and regional exploration criteria for gold mineralization in the Altaid Orogenic Collage: the Tien-Shan province as a key example. *Soc. Econ. Geol. Spec. Publ.* **9**, 177–201.

Zairi, N.M., Kryazhev, S.G., Syngaevskij, E.D., 1995. Role of organic matter of black shales in formation of gold ores. In: *Abstracts of the 16 Symposium Geochemistry of Isotopes*. Geochi, Moscow, pp. 89–90 (in Russian).

Zakharevich, K.V., Kotov, N.V., Vaganov, P.A., Kol'cov, A.B., Donskikh, A.V., 1987. *Gold–Silver Metasomatites in Back Shales*. Leningrad University, Leningrad, 252 p. (in Russian).

Zonenshain, L.P., Kuzmin, M.I., Natapov, L.M., 1990. Geology of the USSR: a plate tectonic synthesis. *American Geophysical Union, Geodynamics Series Monograph* **21**.